Copy 258
RM L54G26a

NACA

RESEARCH MEMORANDUM

AN INVESTIGATION OF A SUPERSONIC AIRCRAFT CONFIGURATION HAVING A TAPERED WING WITH CIRCULAR-ARC SECTIONS AND 40° SWEEPBACK

STATIC LONGITUDINAL AND LATERAL STABILITY AND CONTROL CHARACTERISTICS AT A MACH NUMBER OF 1.89

By M. Leroy Spearman and Edward B. Palazzo

Langley Aeronautical Laboratory
Langley Field, Va.

NATIONAL ADVISORY COMMITTEE FOR AERONAUTICS

WASHINGTON

October 18, 1954

NATIONAL ADVISORY COMMITTEE FOR AERONAUTICS

RESEARCH MEMORANDUM

AN INVESTIGATION OF A SUPERSONIC AIRCRAFT CONFIGURATION HAVING A TAPERED WING WITH CIRCULAR-ARC SECTIONS AND 40° SWEEPBACK

STATIC LONGITUDINAL AND LATERAL STABILITY AND CONTROL CHARACTERISTICS AT A MACH NUMBER OF 1.89

By M. Leroy Spearman and Edward B. Palazzo

SUMMARY

An investigation has been conducted in the Langley 4- by 4-foot supersonic pressure tunnel to determine the static stability and control characteristics of a supersonic aircraft configuration at a Mach number of 1.89. The model had a 40° sweptback tapered wing with 10-percent-thick circular-arc sections normal to the quarter-chord line.

The results indicated a high degree of longitudinal stability with a static margin of about 32 percent of the wing mean aerodynamic chord and positive directional and lateral stability through an angle-of-attack range up to 12°. At an angle of attack of 0°, the results indicated positive effective dihedral and a restoring moment in yaw throughout an angle-of-sideslip range up to 44°.

A comparison of the present results with the results of previous investigations at Mach numbers of 1.40 and 1.59 indicate that for a stabilizer deflection of -10° a decrease in the maximum trim lift coefficient with increasing Mach number occurs; but, because of a more rapid decrease in the lift coefficient required for trimmed level flight, an increase in maneuverability would be available with increasing Mach number. Positive stick position stability was indicated in that a downward deflection of the stabilizer was required for trim with increasing Mach number.

A decrease in directional stability indicated with increasing Mach number may constitute a problem of primary concern.

INTRODUCTION

A comprehensive wind-tunnel investigation has been conducted in the Langley 4- by 4-foot supersonic pressure tunnel to determine the stability and control characteristics of a supersonic aircraft configuration having a tapered wing with circular-arc sections and 40° sweepback. The static longitudinal stability and control characteristics for a Mach number of 1.40 are presented in reference 1 and for a Mach number of 1.59 in reference 2. The static lateral stability characteristics for Mach numbers of 1.40 and 1.59 are presented in reference 3 while the lateral control characteristics are presented in reference 4. The present paper presents the longitudinal and lateral stability and control characteristics at a Mach number of 1.89 and a comparison is made with some of the results obtained at Mach numbers of 1.40 and 1.59. The results of the present tests were obtained through a large angle range (angles of attack up to 28° and angles of sideslip up to 44°) at a relatively low Reynolds number (0.28×10^{6} based on wing mean aerodynamic chord) for the purpose of simulating the characteristics for flight at extremely high altitudes.

COEFFICIENTS AND SYMBOLS

The results of the tests are presented as standard NACA coefficients of forces and moments. The data are referred to the stability axes (fig. 1) with the reference center of gravity at 25 percent of the wing mean aerodynamic chord.

The coefficients and symbols are defined as follows:

C_L lift coefficient, $-Z/qS$

C_X longitudinal-force coefficient, X/qS

C_m pitching-moment coefficient, $M'/qS\bar{c}$

C_Y lateral-force coefficient, Y/qS

C_n yawing-moment coefficient, N'/qSb

C_l rolling-moment coefficient, L'/qSb

Z force along Z-axis

X force along X-axis

M'	moment about Y-axis
Y	force along Y-axis
N'	moment about Z-axis
L'	moment about X-axis
q	free-stream dynamic pressure
S	total wing area
W/S	wing loading, lb/sq ft
$\bar{c}$	wing mean aerodynamic chord, $\frac{2}{S}\int_0^{b/2} c^2 dy$
c	airfoil section chord
b	wing span
g	acceleration due to gravity, ft/sec^2
h	altitude, ft
M	Mach number
L/D	ratio of lift to drag ($C_L/-C_X$ at $\beta = 0^\circ$)
ϵ	effective angle of downwash, deg
α	angle of attack of fuselage center line, deg
β	angle of sideslip, deg
i_t	stabilizer incidence angle with respect to fuselage center line, deg
δ_r	rudder deflection, deg
δ_a	aileron deflection, deg (subscript L or R refers to left or right aileron)
n_p	neutral-point location, percent $\bar{c}$
n_o	tail-off aerodynamic-center location, percent $\bar{c}$

$C_{L_{\alpha}}$ lift-curve slope

C_{m_t} increment of pitching-moment coefficient provided by horizontal tail

$C_{m_{C_L}}$ rate of change of pitching-moment coefficient with lift coefficient at $C_m \approx 0$

$\frac{\partial C_m}{\partial i_t}$ rate of change of pitching-moment coefficient with stabilizer incidence angle at constant angle of attack

$\frac{\partial \epsilon}{\partial \alpha}$ rate of change of effective downwash angle with angle of attack

C_{X_o} minimum longitudinal-force coefficient with tail off

$\alpha_{C_L=0}$ angle of attack for zero lift with tail off

$C_{Y_{\beta}}$ rate of change of lateral-force coefficient with angle of sideslip

$C_{n_{\beta}}$ rate of change of yawing-moment coefficient with angle of sideslip

$C_{l_{\beta}}$ rate of change of rolling-moment coefficient with angle of sideslip

$C_{n_{\delta_r}}$ rate of change of yawing-moment coefficient with rudder deflection

$C_{l_{\delta_a}}$ rate of change of rolling-moment coefficient with aileron deflection

$\Delta C_X/C_L^2$ longitudinal force due to lift

ΔC_X increment of longitudinal-force coefficient above minimum

MODEL AND APPARATUS

A three-view drawing of the model is shown in figure 2 and the geometric characteristics of the model are presented in table I. A photograph of the configuration is shown in figure 3.

The model had a wing swept back 40° at the quarter-chord line, an aspect ratio of 4, a taper ratio of 0.5, and 10-percent-thick circular-arc airfoil sections normal to the quarter-chord line. Flat-sided 20-percent-chord ailerons having a trailing-edge thickness 0.5 of the hinge-line thickness were installed on the outboard 50 percent of the wing semispans.

Deflections of the stabilizer were controlled remotely through the use of an electric motor mounted inside the model fuselage. Deflections of the ailerons and rudder were set manually.

Force and moment measurements were made through the use of a six-component internal strain-gage balance.

TESTS AND CORRECTIONS

Test Conditions

The conditions for the tests were:

Mach number	1.89
Reynolds number, based on $\bar{c}$	0.28×10^6
Stagnation pressure, lb/sq in. abs.	2
Stagnation temperature, °F	100

Corrections and Accuracy

The tests were made in the $M = 2$ nozzle which, for pressures above 4 lb/sq in. abs., produces a Mach number of 2.01. However, based upon a recent nozzle calibration for a stagnation pressure of 2 lb/sq in. abs., it was determined that the test section Mach number was 1.89 ± 0.02. The base pressure was measured and the chord force was adjusted by equating the base pressure to the free-stream static pressure. The angles of attack and sideslip were corrected for the deflection of the balance and sting under load.

The estimated errors in the individual measured quantities are as follows:

C_L	± 0.005
C_X	± 0.002
C_m	± 0.002
C_Y	± 0.003

C_n	± 0.0002
C_l	± 0.0002
α, deg	± 0.1
β, deg	± 0.1
i_t, deg	± 0.1
δ_a, deg	± 0.1
δ_r, deg	± 0.1

RESULTS AND DISCUSSION

Longitudinal Stability and Control

Aerodynamic characteristics in pitch for the complete model with various values of i_t as well as for the model with the horizontal tail removed are presented in figure 4. The lift and moment curves indicate a static margin of about $0.32\bar{c}$. Above $\alpha \approx 18^{\circ}$, C_{L_α} decreases and $-C_{m_{C_L}}$ increases. The change in $-C_{m_{C_L}}$ is apparently an effect of the wing downwash on the horizontal tail since the values of $-C_{m_{C_L}}$ when the horizontal tail is off indicates no increase in slope at the higher angles of attack.

The variation of i_t, L/D, and α with C_L for trimmed flight is shown in figure 5. The results obtained at Mach numbers of 1.40 and 1.59 (refs. 1 and 2, respectively) are included for comparison. The decrease in C_{L_α} with increasing Mach number is apparent and a decreased stabilizer effectiveness with increasing Mach number is indicated. The maximum values of L/D decrease slightly with increasing Mach number, but, at the lower lift coefficients (below $C_L \approx 0.17$) that may be required for level flight at high altitudes, the values of L/D increase slightly with increasing Mach number. Even the maximum values of L/D obtained are, however, quite low.

The variation of i_t with C_L for trimmed level flight at $M = 1.40$, 1.59, and 1.89 is repeated in figure 6 and includes the variation of i_t for trim with Mach number and indicates the maximum maneuverability available for a wing loading of 50 pounds per square foot at an altitude of 60,000 feet. The variation of i_t for trim with Mach number indicates stick position stability, that is, a forward movement of the stick (stabilizer trailing edge down) is required to trim with increasing Mach number. The maximum maneuverability available (assuming a maximum value for i_t of -10°) increases with increasing Mach number regardless of the decrease in maximum trim C_L since the C_L required for level flight decreases at a greater rate.

There is a decrease in the magnitude $\partial C_m/\partial i_t$ with increasing Mach number as well as a general decrease in $\partial\epsilon/\partial\alpha$ (fig. 7). The effective downwash ϵ was obtained from figure 4 by use of the relation $\epsilon = \alpha + i_t - \dfrac{C_{m_t}}{\partial C_m/\partial i_t}$. The longitudinal force due to lift $\Delta C_X/{C_L}^2$ increases with increasing Mach number (fig. 8) in a manner that might be anticipated from the decrease in C_{L_α}.

Lateral Stability and Control

The variations of C_n, C_l, and C_Y with sideslip are fairly linear up to $\beta \approx 8^{\circ}$ but are somewhat nonlinear throughout the range from $\beta \approx 8^{\circ}$ to $\beta \approx 44^{\circ}$ (fig. 9). The slope C_{n_β} is quite small or even negative in the range from $\beta \approx 10^{\circ}$ to $\beta \approx 30^{\circ}$ although a restoring moment (for $\delta_r = 0^{\circ}$) remains available throughout the range. Removal of the horizontal tail considerably decreased the magnitude of the restoring moment in yaw in the angle-of-sideslip range above 15°. This may result either from the loss of a yawing-moment increment produced by the horizontal tail itself or from a resultant forward shift in the effective center of pressure of the vertical tail since the lateral-force measurements indicate an increase in the effectiveness of the vertical tail upon removal of the horizontal tail.

A rudder deflection of -30.5° indicates a trim angle of sideslip of only about -4° (fig. 9).

The tail-off configuration shows essentially no rolling-moment variation with sideslip but the addition of the vertical tail results in a positive effective dihedral. Removal of the horizontal tail had little effect on the rolling-moment increment produced by the vertical tail.

There is little variation of C_X with β for all configurations (fig. 9). It should be pointed out that the reference longitudinal axis for the stability axis system is fixed in sideslip with the body axis; hence, the values of C_X do not represent the true drag with respect to the wind direction. The drag force might be obtained by properly combining the components of C_X and C_Y in the wind axis direction.

The lift remains essentially constant for all configurations up to $\beta \approx 16^{\circ}$ at $\alpha = 0^{\circ}$ and then progressively decreases. The pitching moment for the complete model indicates a continual increase in the negative moment up to $\beta \approx 28^{\circ}$ and then a decrease in the negative moment. This variation is apparently related to the effect of the wing wake on the horizontal tail since the variation is much less pronounced for the model with the horizontal tail off and is even less noticeable for the model with both the vertical and horizontal tails removed. The variation of C_m with β appears to be slightly greater at $\alpha = 4^{\circ}$ than at $\alpha = 0^{\circ}$ possibly because of the greater proximity of the horizontal tail to the wing wake.

The incremental contributions of the tail (horizontal and vertical) to C_n, C_l, and C_Y (fig. 9) continue to increase throughout the angle-of-sideslip range. An inspection of the horizontal-tail-off results indicates that the tail increments would be more linear without the horizontal tail.

The variation with angle of attack of C_n, C_l, and C_Y at a constant β of 4° for an i_t of 0° and -8° (fig. 10) serves as an indication of the effect of α and i_t on the slopes $C_{n_{\beta}}$, $C_{l_{\beta}}$, and $C_{Y_{\beta}}$. There is a slight decrease indicated for $C_{n_{\beta}}$ and an increase in $-C_{l_{\beta}}$ with increasing angle of attack. There is no effect of i_t indicated for $C_{n_{\beta}}$ but a slight decrease in the effective dihedral $\left(-C_{l_{\beta}}\right)$ occurs when the tail setting is changed from 0° to -8°. There is essentially no effect of α or i_t on the variation of $C_{Y_{\beta}}$.

The rolling-moment and yawing-moment coefficients resulting from a $\pm 10^{\circ}$ aileron deflection $\left(\delta_{a_L} = 10^{\circ},\ \delta_{a_R} = -10^{\circ}\right)$ are shown in figure 11. The adverse yawing-moment coefficient increases with angle of attack until at $\alpha \approx 16^{\circ}$ the yawing-moment coefficient caused by the ailerons is about equal to that produced by the full rudder deflection of -30.5°.

The directional control effectiveness of the rudder deflected -30.5° is essentially constant with angle of attack. The rolling-moment produced by the rudder is about one-half of that produced by $\delta_a = \pm 10^{\circ}$ at $\alpha = 0^{\circ}$ (fig. 11).

Variation of Aerodynamic Parameters With Mach Number

A summary showing the variation of various aerodynamic parameters with Mach number as obtained from the investigations performed in the

Langley 4- by 4-foot supersonic pressure tunnel is presented in figure 12 (refs. 1 to 4 and present tests). The slope values shown were measured near α and β of 0°. The results obtained at $M = 1.89$ may be used to supplement the correlation of results for the Mach number range up to 2.4 as presented in reference 5. Of primary concern, for configurations of the type considered, is the decreasing vertical-tail lift-curve slope with Mach number and the corresponding decrease in directional stability $\left(C_{n_{\beta}}\right)$. Control effectiveness also shows a characteristic decrease through the Mach number range considered but whether or not this constitutes a problem depends upon the attendant changes in the stability and consequently in the control requirements.

CONCLUSIONS

The results of a stability and control investigation at a Mach number of 1.89 of a model of a supersonic aircraft configuration indicated the following conclusions:

1. A high degree of static longitudinal stability was indicated with a static margin of about 32 percent of the wing mean aerodynamic chord.

2. The configuration indicated positive directional stability and positive dihedral effect through an angle-of-attack range up to 12°. At an angle of attack of 0°, positive effective dihedral and a restoring moment in yaw were indicated throughout an angle-of-sideslip range up to 44°.

3. Positive lateral and directional control was maintained through an angle-of-attack range up to 16°.

A comparison of the present results with the results of previous investigations at Mach numbers of 1.40 and 1.59 indicated the following conclusions:

1. Although the maximum trim lift coefficient (stabilizer deflection of -10°) decreased with increasing Mach number, the maneuvering ability increased since the lift coefficient required for trimmed flight decreased with Mach number at a greater rate than did the maximum lift coefficient.

2. Positive stick position stability was indicated in that a downward deflection of the stabilizer was required for trim with increasing Mach number.

3. A decrease in directional stability indicated with increasing Mach number may constitute a problem of primary concern.

Langley Aeronautical Laboratory,
National Advisory Committee for Aeronautics,
Langley Field, Va., January 6, 1954.

REFERENCES

1. Spearman, M. Leroy: An Investigation of a Supersonic Aircraft Configuration Having a Tapered Wing With Circular-Arc Sections and 40° Sweepback - Static Longitudinal Stability and Control Characteristics at a Mach Number of 1.40. NACA RM L9L08, 1950.

2. Spearman, M. Leroy, and Hilton, John H., Jr.: An investigation of a Supersonic Aircraft Configuration Having a Tapered Wing With Circular-Arc Sections and 40° Sweepback - Static Longitudinal Stability and Control Characteristics at a Mach Number of 1.59. NACA RM L50E12, 1950.

3. Spearman, M. Leroy: An Investigation of a Supersonic Aircraft Configuration Having a Tapered Wing With Circular-Arc Sections and 40° Sweepback - Static Lateral Stability Characteristics at Mach Numbers of 1.40 and 1.59. NACA RM L50C17, 1950.

4. Robinson, Ross B.: An Investigation of a Supersonic Aircraft Configuration Having a Tapered Wing With Circular-Arc Sections and 40° Sweepback - Static Lateral Control Characteristics at Mach Numbers of 1.40 and 1.59. NACA RM L50I11, 1950.

5. Spearman, M. Leroy, and Robinson, Ross B.: The Aerodynamic Characteristics of a Supersonic Aircraft Configuration With a 40° Sweptback Wing Through a Mach Number Range From 0 to 2.4 As Obtained From Various Sources. NACA RM L52A21, 1952.

TABLE I.- GEOMETRIC CHARACTERISTICS OF MODEL

Wing:	
Area, sq ft	1.158
Aspect ratio	4
Sweepback of quarter-chord line, deg	40
Taper ratio	0.5
Mean aerodynamic chord	0.557
Airfoil section normal to quarter-chord line	10-percent-thick circular-arc
Twist, deg	0
Horizontal tail:	
Area, sq ft	0.196
Aspect ratio	3.72
Sweepback of quarter-chord line, deg	40
Taper ratio	0.5
Airfoil section	NACA 65-008
Vertical tail:	
Area (exposed), sq ft	0.172
Aspect ratio (based on exposed area and span)	1.17
Sweepback of leading edge, deg	40.6
Taper ratio	0.337
Airfoil section, root	NACA 27-010
Airfoil section, tip	NACA 27-008
Fuselage:	
Fineness ratio (neglecting canopies)	9.4
Miscellaneous:	
Tail length from $\bar{c}/4$ wing to $\bar{c}_t/4$ tail, ft	0.917
Tail height, wing semispans above fuselage center line	0.153

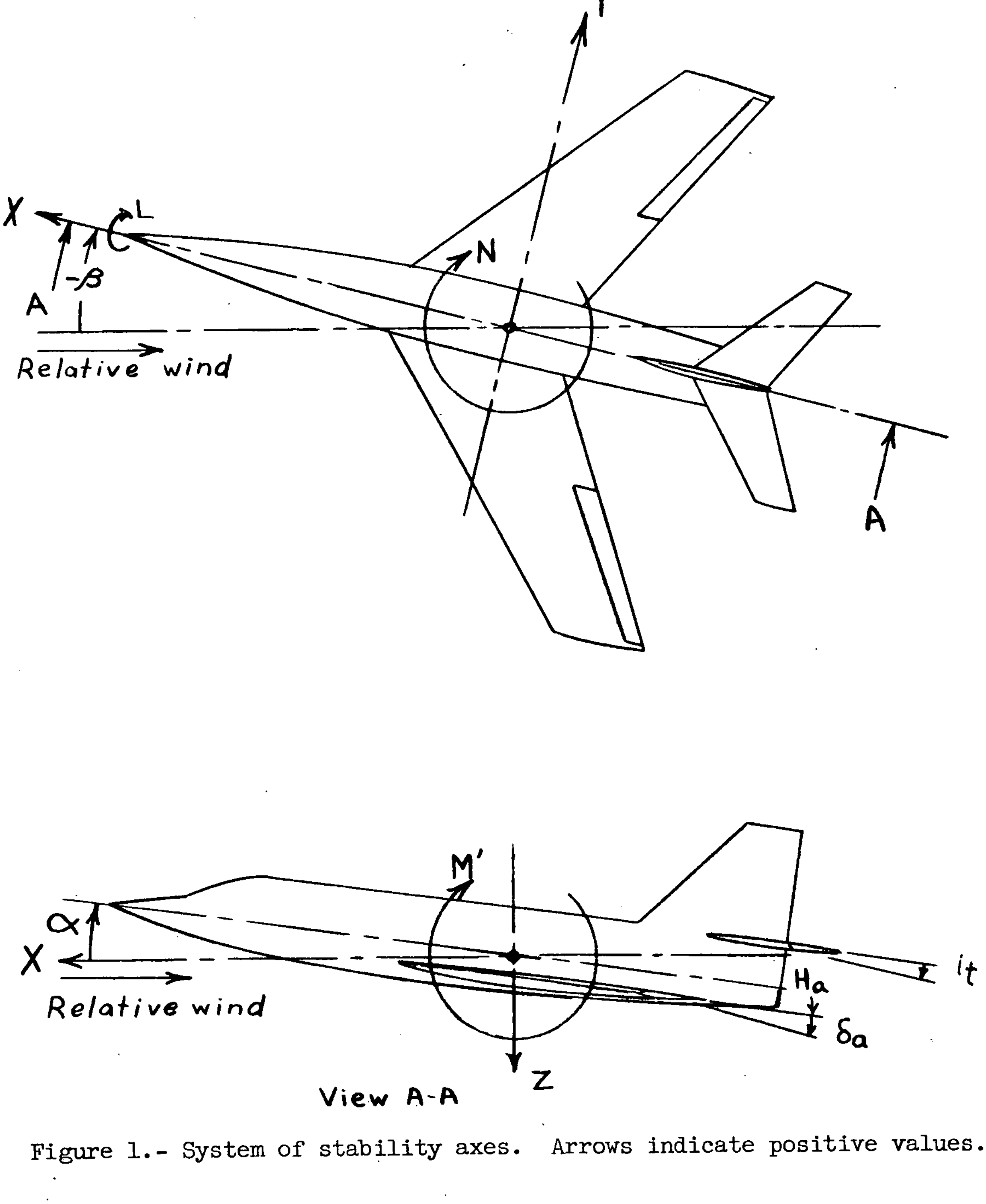

Figure 1.- System of stability axes. Arrows indicate positive values.

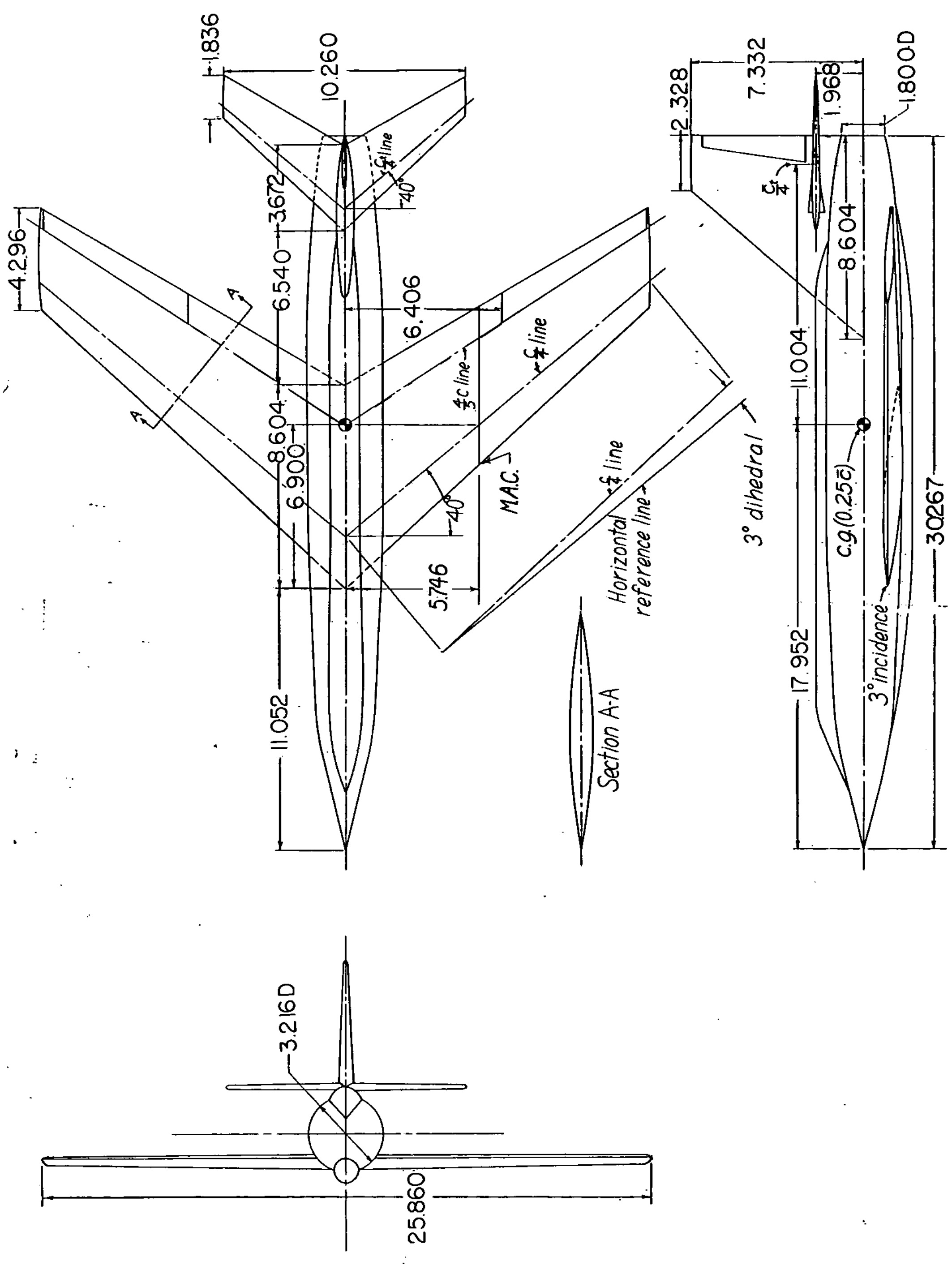

Figure 2.- Details of model of supersonic aircraft configuration. Dimensions in inches unless otherwise noted.

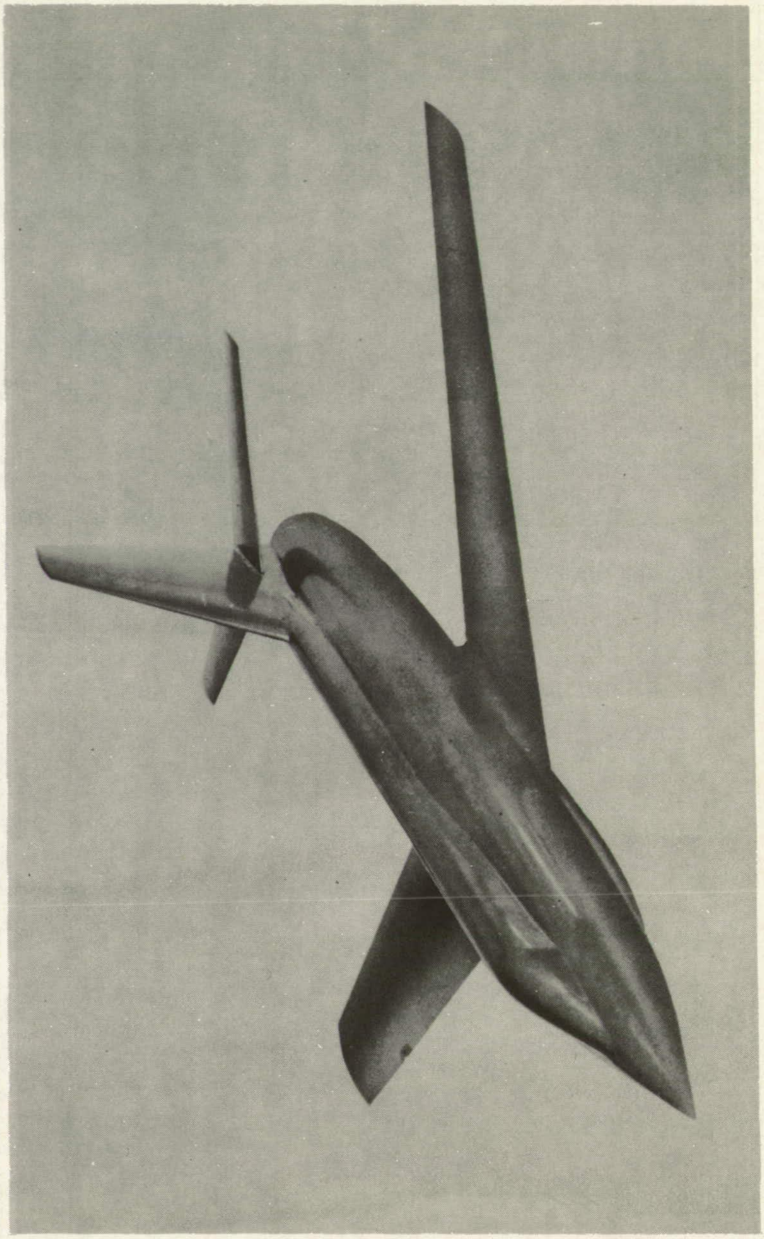

L-64078.1

Figure 3.- Photograph of model.

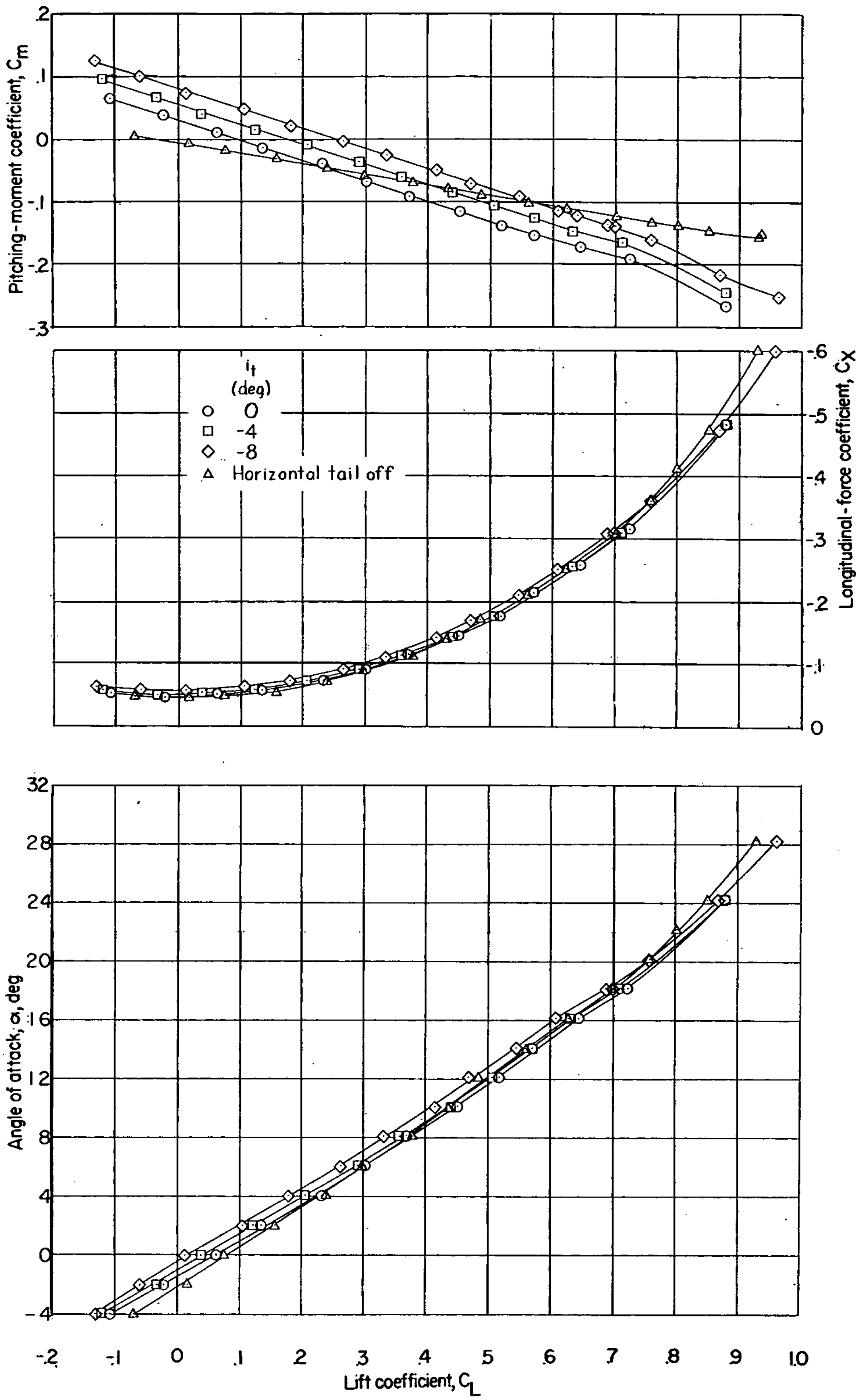

Figure 4.- Aerodynamic characteristics in pitch. M = 1.89.

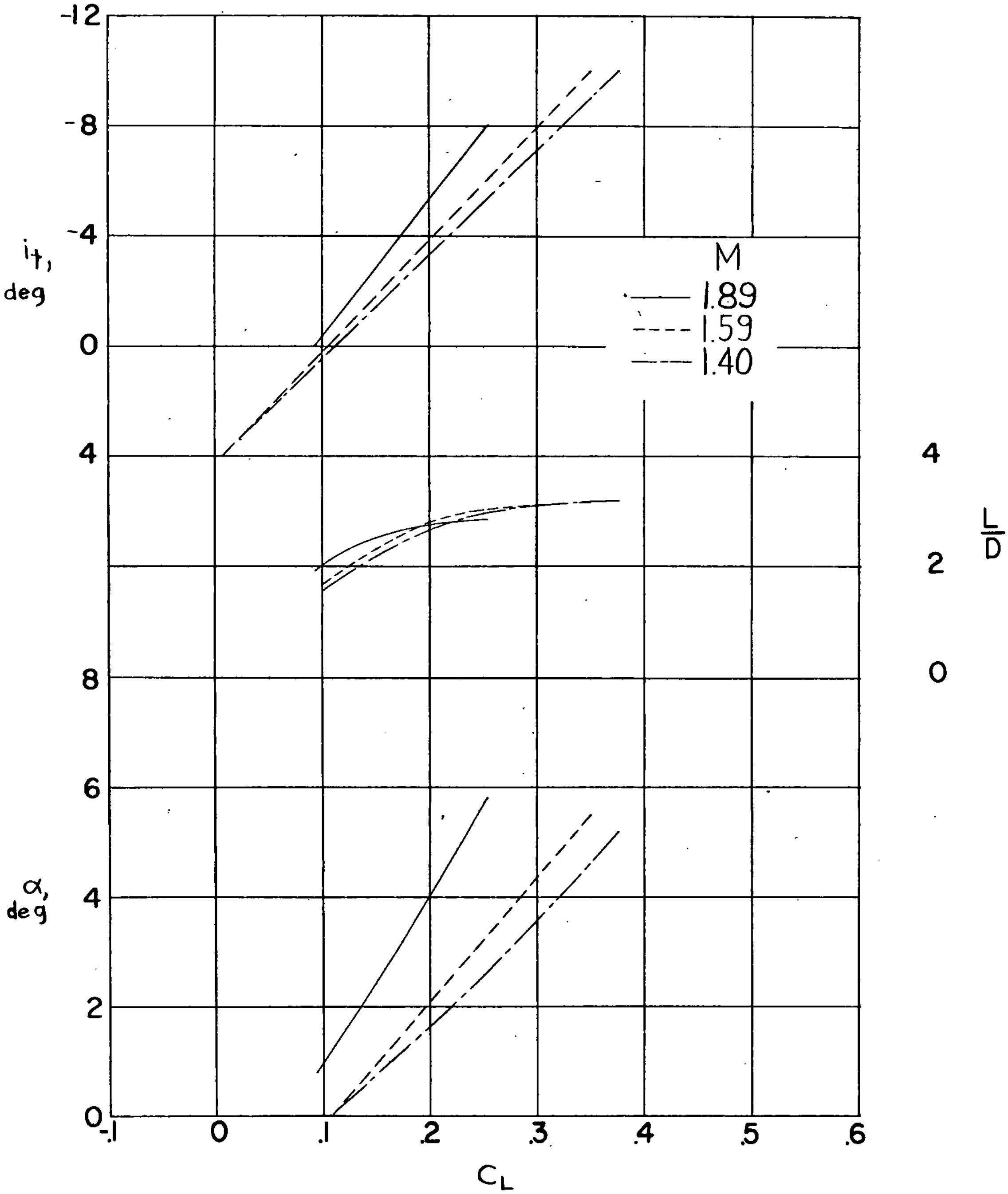

Figure 5.- Variation of trim longitudinal characteristics with lift coefficient for various Mach numbers.

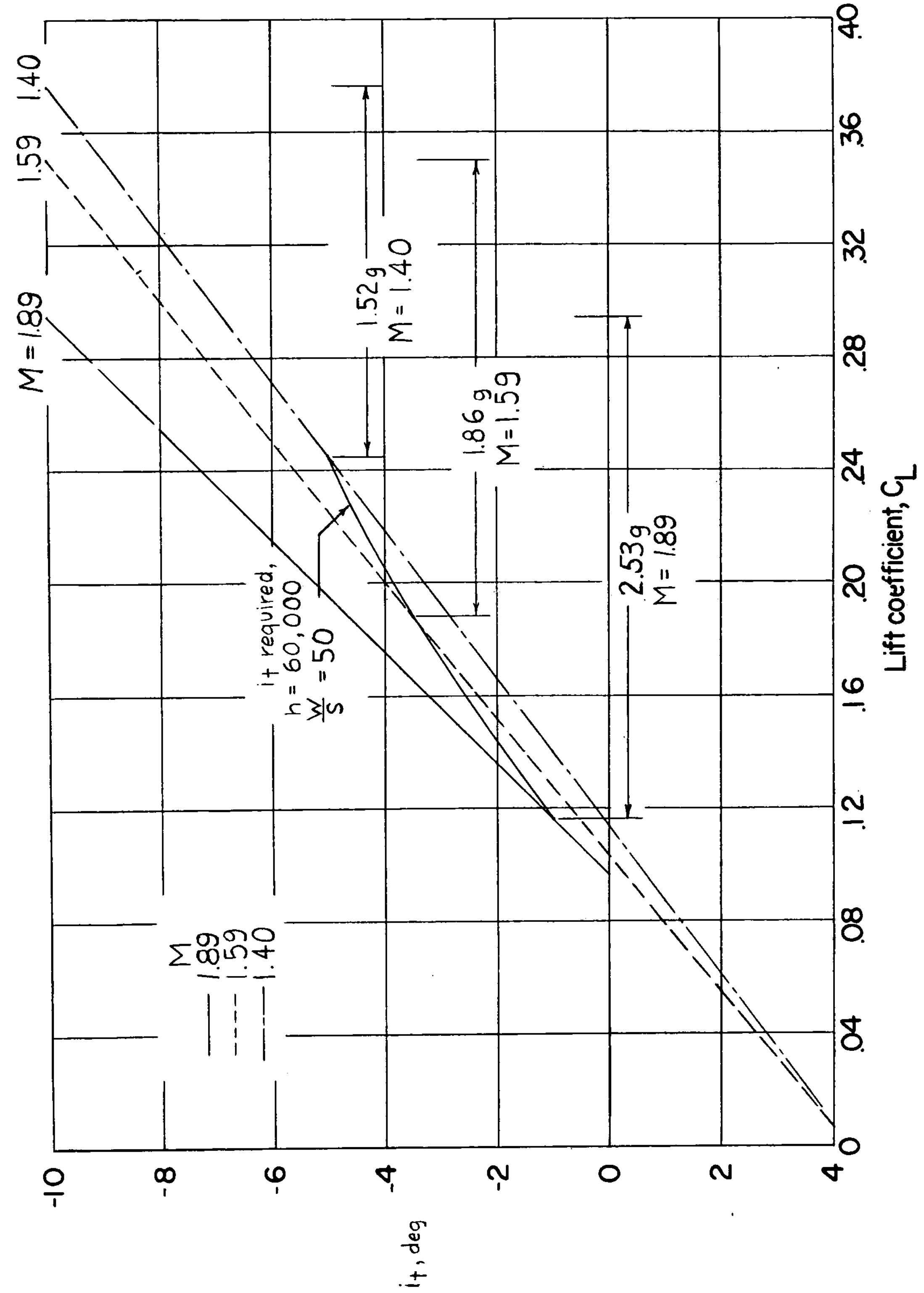

Figure 6.- Longitudinal control characteristics for various Mach numbers.

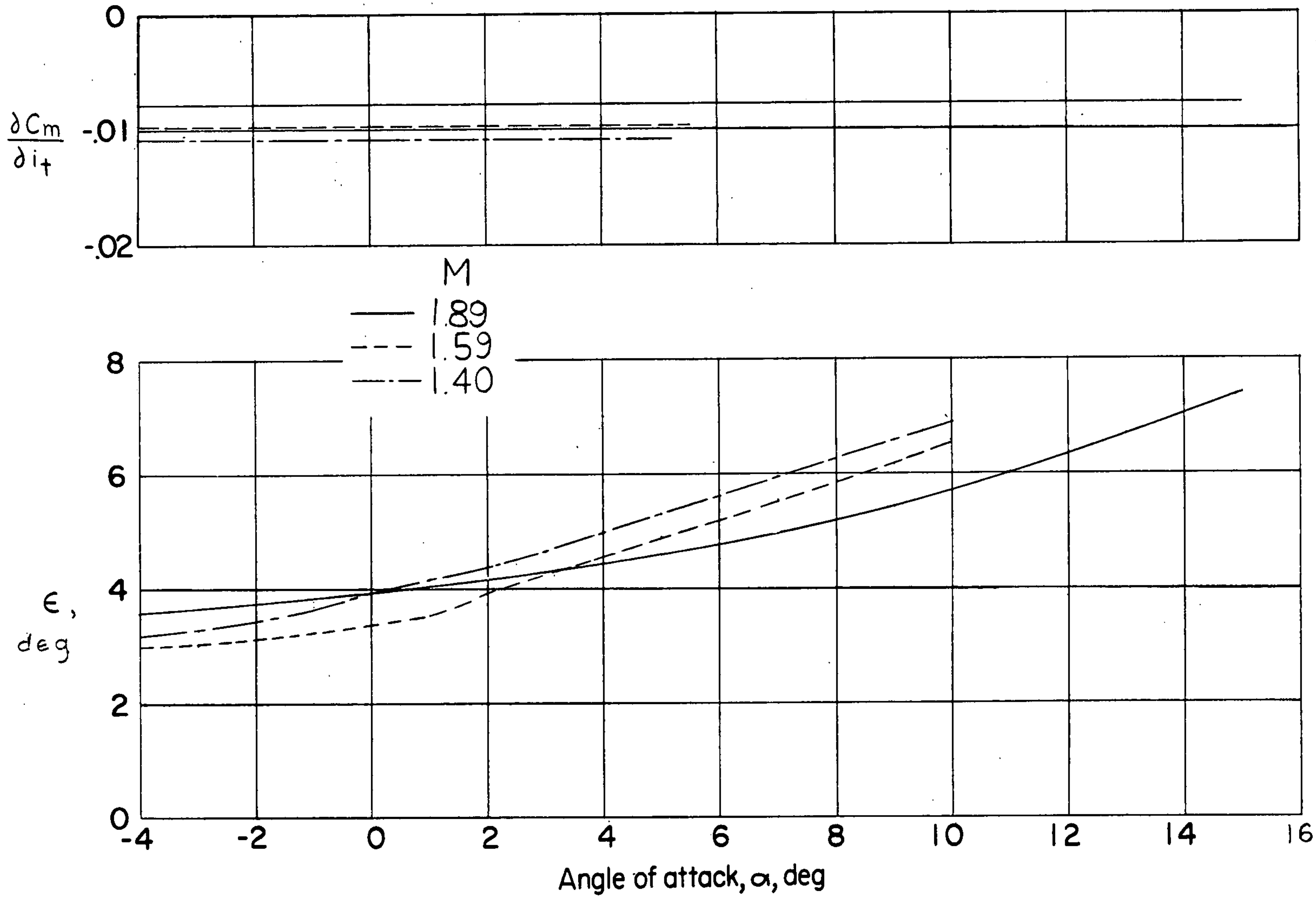

Figure 7.- Variation of stabilizer effectiveness and effective downwash angle with angle of attack and Mach number.

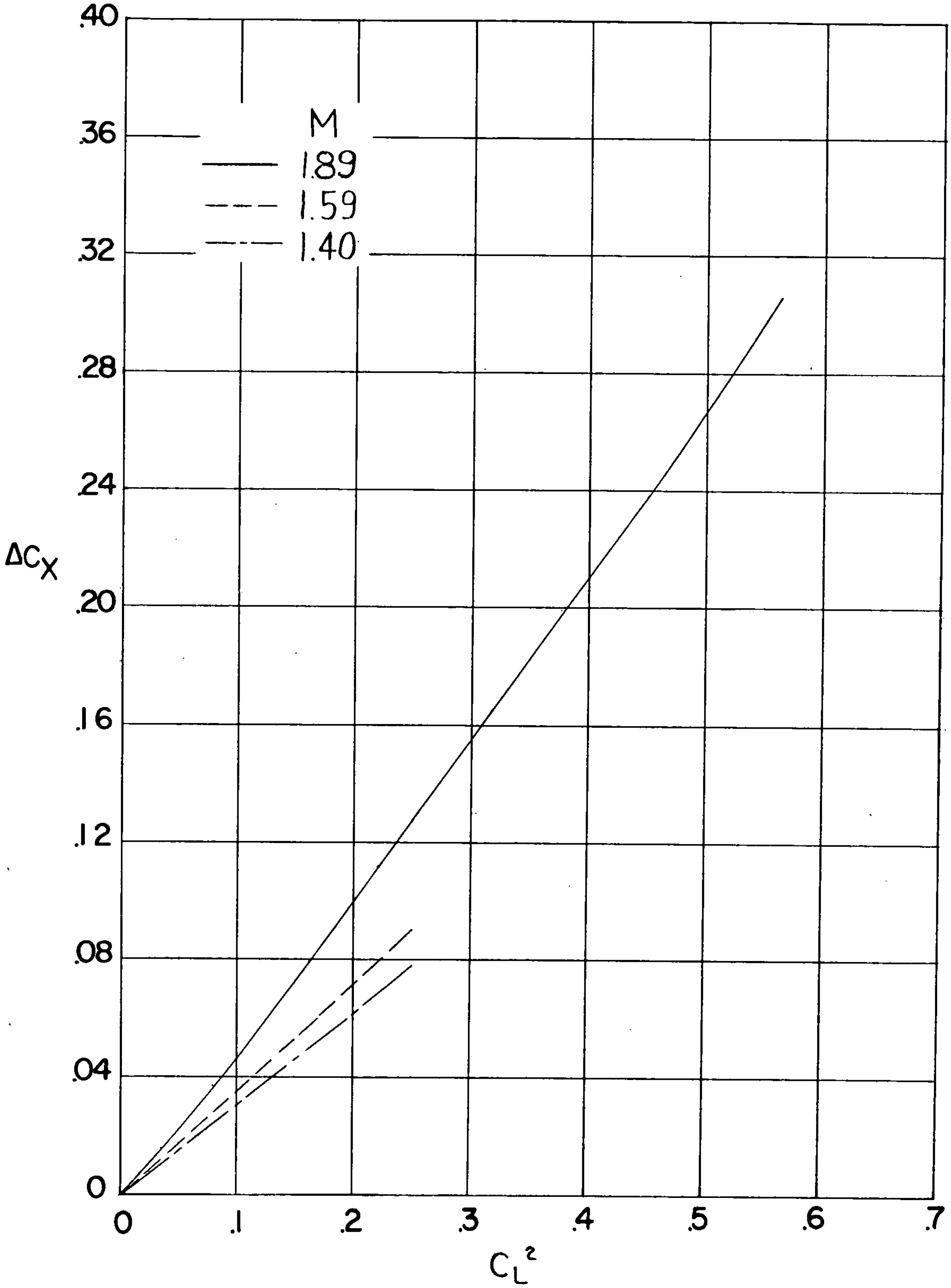

Figure 8.- Variation of drag due to lift for various Mach numbers. $i_t = 0^\circ$.

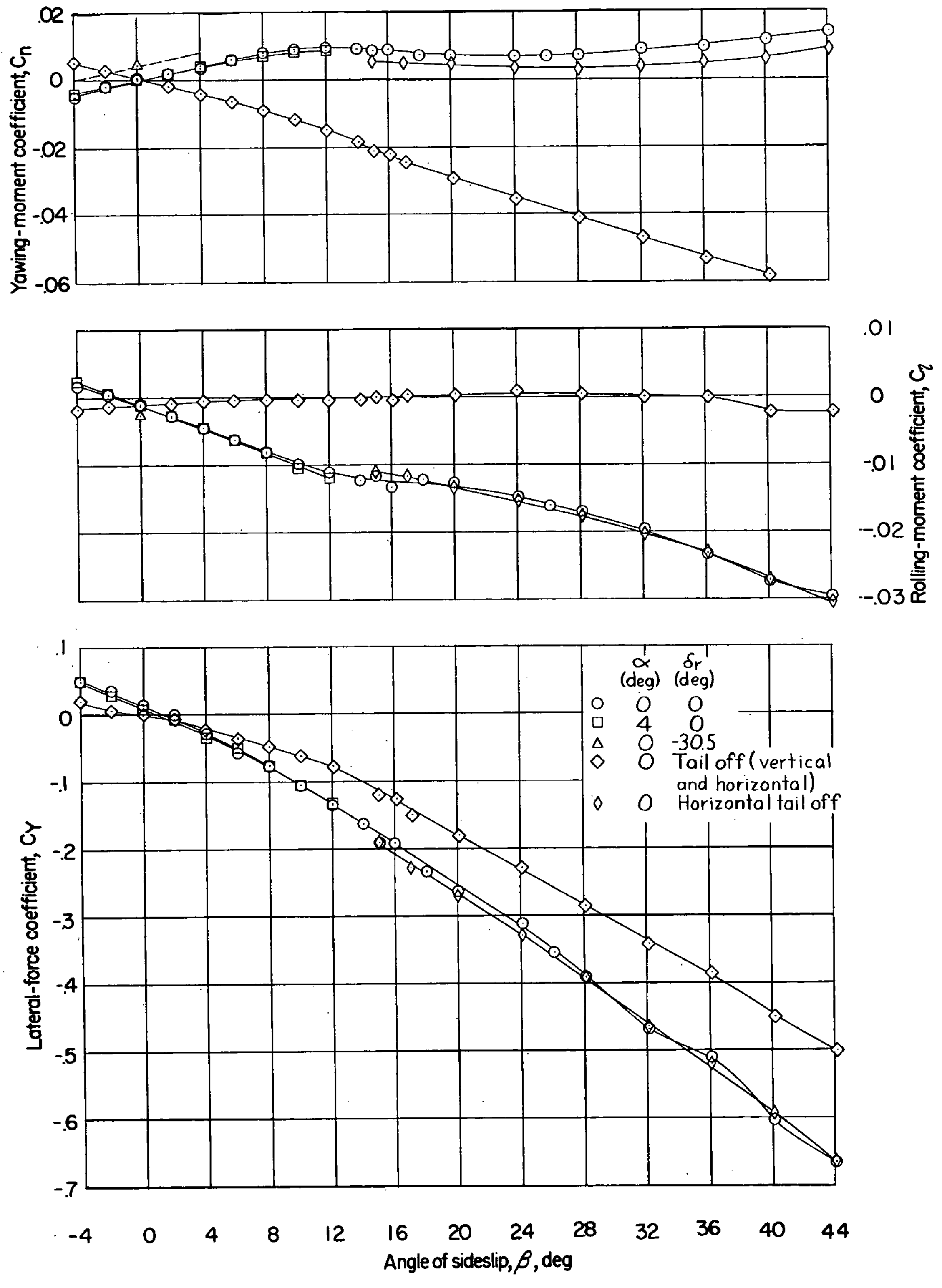

Figure 9.- Aerodynamic characteristics in sideslip for various configurations. M = 1.89.

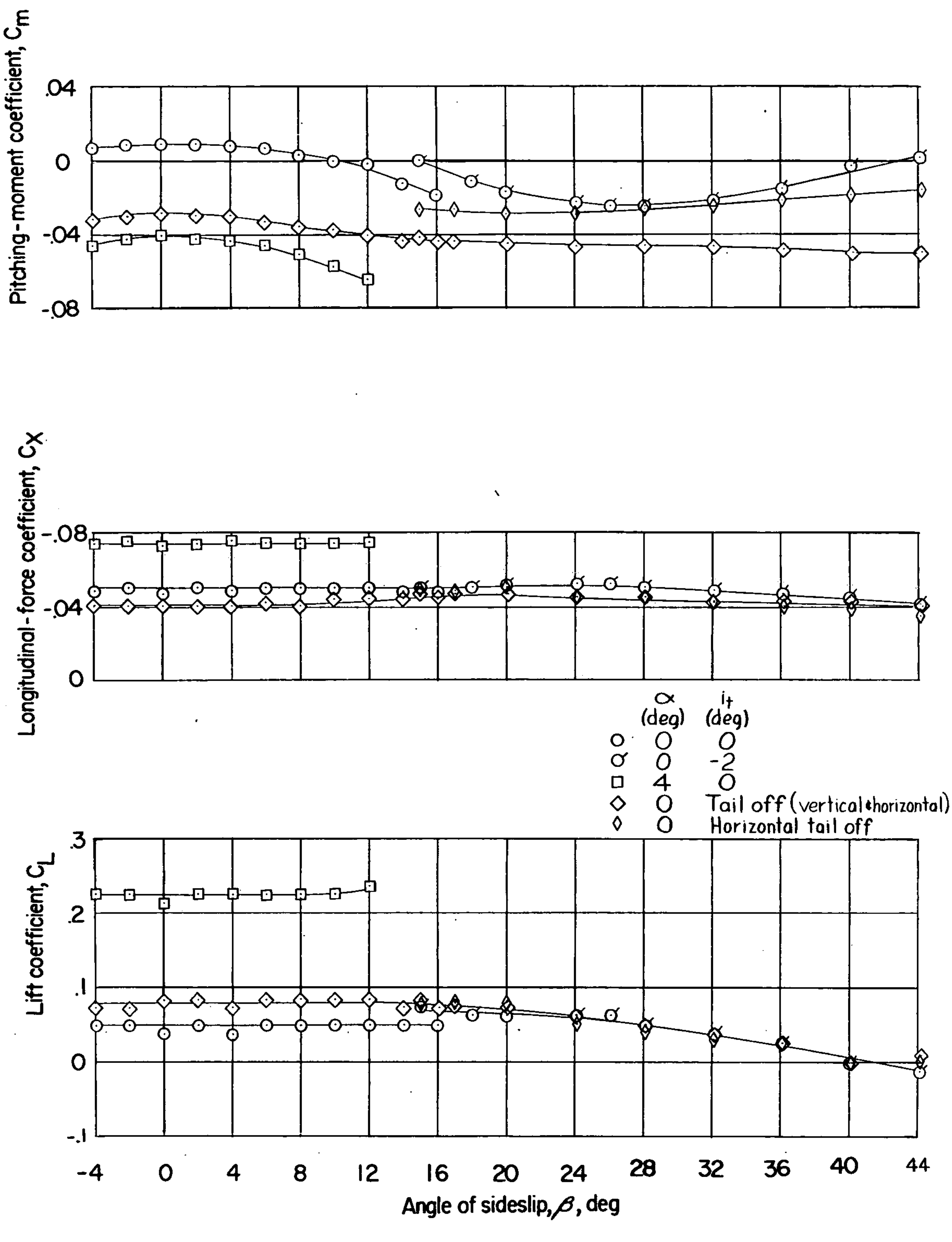

Figure 9.- Concluded.

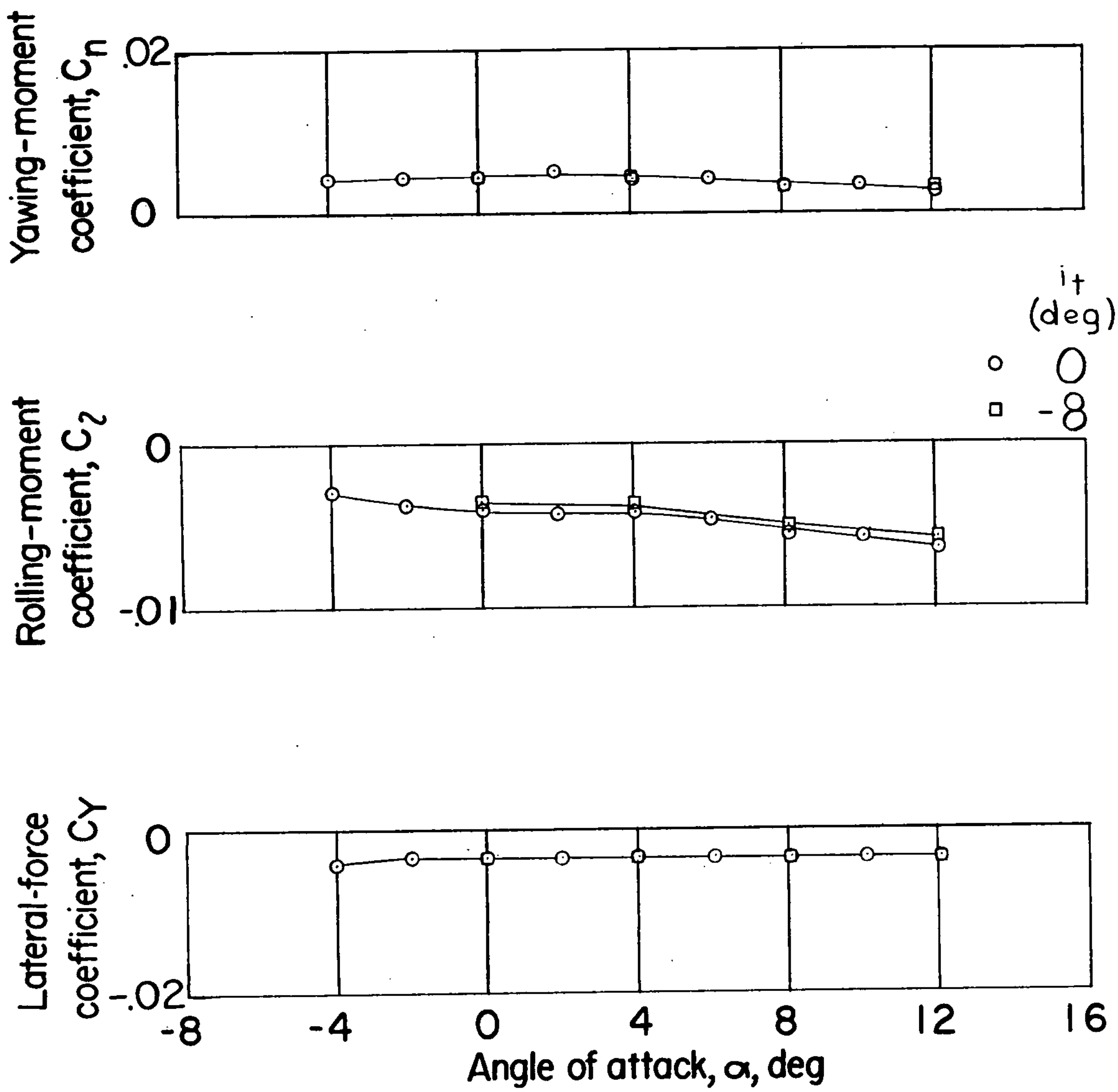

Figure 10.- Effect of angle of attack and stabilizer incidence on the lateral derivatives at $\beta = 4^\circ$. M = 1.89.

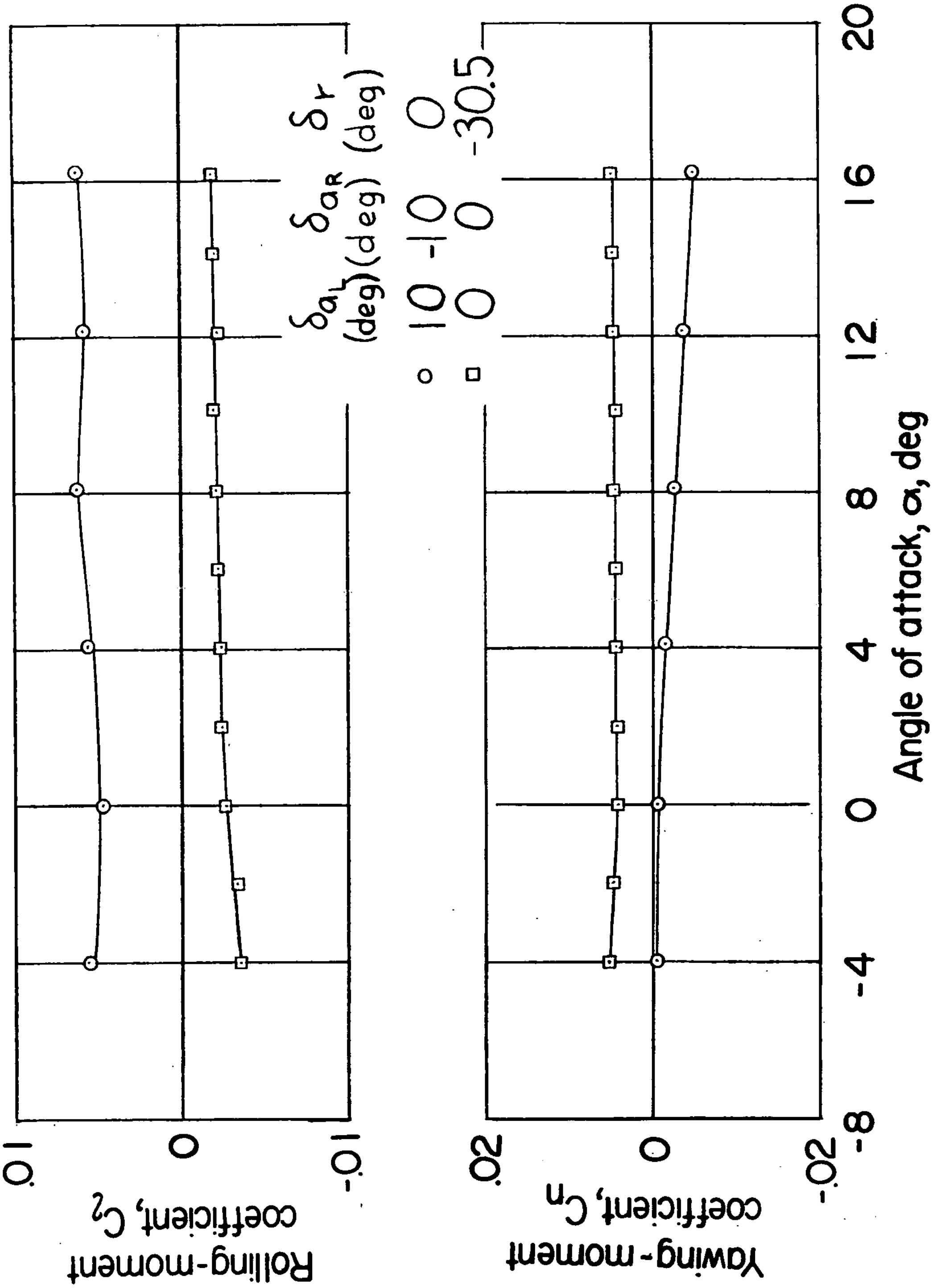

Figure 11.- Effect of angle of attack on the aileron and rudder control effectiveness. M = 2.01.

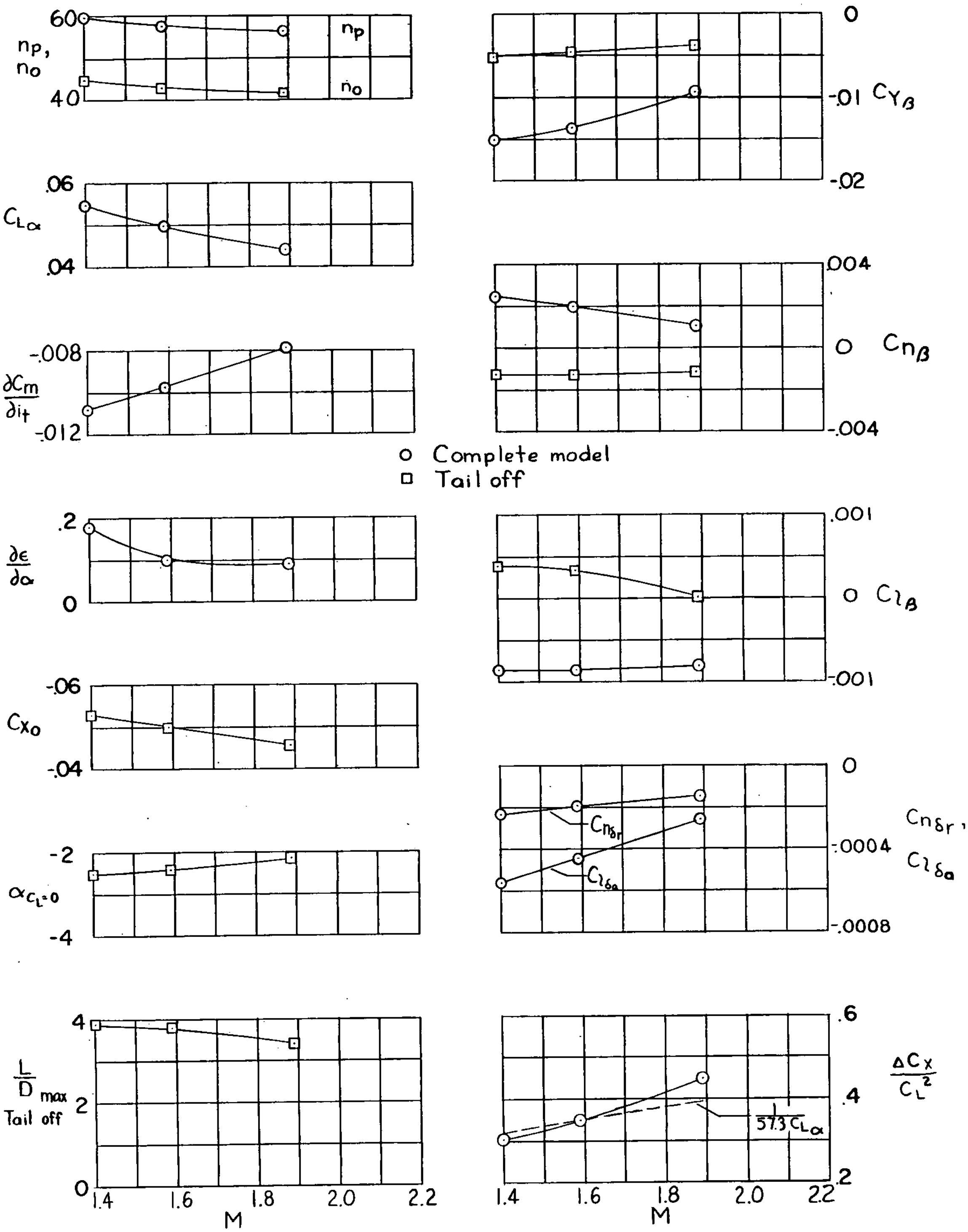

Figure 12.- Variation of various aerodynamic characteristics with Mach number.

NACA-Langley - 10-18-54 - 350

CONFIDENTIAL

CONFIDENTIAL